

An Achievable and Analytic Solution to Information Bottleneck for Gaussian Mixtures

Yi Song, Kai Wan, *Member, IEEE*, Zhenyu Liao, *Member, IEEE*,
Giuseppe Caire *Fellow, IEEE*

Abstract

The information bottleneck (IB) approach, initially introduced by Tishby *et al.* to assess the “compression–relevance” tradeoff for a remote source coding problem in communications, gains popularity recently in its application to modern machine learning (ML). Despite its seemingly simple form, the solution to IB problem remains largely *unknown*, and can *only* be assessed numerically even in the simple setting of Gaussian mixture model that is of fundamental significance in ML. In this paper, by combining ideas of hard quantization and soft nonlinear transformation, we derive *closed-form achievable* bounds for the IB problem under the above setting. The derived bounds establish surprisingly close behavior to the (numerically) optimal IB solution obtained by Blahut–Arimoto (BA) algorithm, on both synthetic and real-world (so non-Gaussian mixture) datasets, suggesting possibly wider applicability of our results.

I. INTRODUCTION

Large-scale machine learning (ML) models, and in particular, deep neural networks (DNNs), have made significant progress over the past decade, with a rapidly growing list of applications ranging from computer vision [1], game [2], to speech and natural language processing [3], as well as AI-generated content [4], to name a few.

Despite their sophisticated and task-specific structures (that help boost the performance to a superhuman level), many basic concepts, design principles, and building blocks of modern ML models are deeply rooted in some simple but highly non-trivial ideas in probability, information

Y. Song and G. Caire are with Faculty of Electrical Engineering and Computer Science, Technical University of Berlin, Berlin, Germany (email: yi.song@tuberlin.de, caire@tu-berlin.de).

K. Wan and Z. Liao are with School of Electronic Information and Communications, Huazhong University of Science and Technology, Wuhan, China (email: kai_wan@hust.edu.cn, zhenyu_liao@hust.edu.cn).

theory (IT), and optimization. As an instance, the concepts of mutual information and cross-entropy are widely used in ML [5, Section 3.13], for features and/or model selection [6], the (loss) design of generative models [7], [8], [9], [10], unsupervised [11] as well as self-supervised [12] learning methods.

In this respect, the information bottleneck (IB) approach introduced in [13], initially proposed to characterize the tradeoff between the compression and the relevance rate for a remote source coding problem, adopts mutual information as the figure of merit. In recent years, IB has received significant research attention in ML, see, for example [14], [15], [16], [17], [18], [19], [20] and the references therein. In plain words, the IB framework describes the procedure of information extraction from a target random variable y through an observable random variable x (that is correlated to y), by forming the Markov chain $y \longrightarrow x \longrightarrow t(x)$, with $t(x)$ a (possibly random) function of x that “extracts” information from the observation x . In the methodology of IB, the extracted information, or the *feature* $t(x)$, is good if it is a “compact” (in an information-theoretic sense) representation of x , and at the same time retains sufficiently rich information about the target y , in such a way that the mutual information $I(x; t)$ is small while $I(y; t)$ remains large; that is, the IB method solves the optimization problem:

$$\begin{aligned} \max_{p(t|x)} \quad & I(y; t) \\ \text{s.t.} \quad & I(x; t) \leq R, \quad \text{given } R \geq 0. \end{aligned} \tag{1}$$

Due to the mathematically involved form of IB, the optimal design of $t(x)$ is known in closed-form only in the case of symmetric Bernoulli or jointly Gaussian (x, y) [19]. For the general case, the (approximated) optimal solution of (1) can be numerically obtained by the Blahut-Arimoto (BA) algorithm in [13]. Apart from numerical evaluations, very little is known beyond the above settings, even for the simple yet most natural Gaussian mixture model that is of direct interest in classification [21]. In this paper, we focus on the IB problem in (1), by considering Bernoulli distributed target y and Gaussian mixture input x , the explicit *and/or* optimal solution of which remains largely open in the community [20].

A. Our contribution

Our main contributions are the following:

- (i) By combing ideas of hard quantization and soft nonlinear transformation, we derive, in Theorem 3, a *closed-form* solution to the open IB problem with Bernoulli source and

Gaussian mixture data. This is, to the best of our knowledge, the first time an achievable *closed-form* solution is proposed under this setting.

- (ii) Numerical experiments on both synthetic Gaussian mixture and real-world non-Gaussian data are performed, showing the satisfactory performance of the proposed analytic IB scheme when compared to numerical algorithms, including the (approximated) optimal Blahut-Arimoto (BA) algorithm in [13] and the popular Information Dropout approach [22] based on simple neural networks.

B. Related works

Here, we provide a brief review of related previous efforts.

a) IB and its applications in ML.: Although first applications of the IB formulation to ML, e.g., for clustering [23], date two decades ago, it is quickly gaining popularity recently with the rapid growth of deep learning. From a theoretical perspective, IB is used to analyze or explain the training of, e.g., DNN models, to justify the choice of network depth, structure, activation function, and/or optimizer [14], [16]; from a more practical standpoint, IB serves as an optimization objective to enhance generalization, robustness to adversarial examples [15], sufficiency and/or disentanglement of representations [22]. We refer the readers to [20] for a review of IB and its applications in ML.

An information-theoretic problem closely related to the IB is privacy funnel (PF) [24]. With the Markov chain $y \rightarrow x \rightarrow t(x)$, the PF problem seeks to extract a representation $t(x)$ from the data x , where the leakage rate of y observing $t(x)$ is minimized while the relevance between $t(x)$ and x is no less than a given number. Obviously, the optimal PF rate is a lower bound of the IB rate [25], [26]. The PF (and similarly IB) problem finds its application in secrecy preserving and fair ML [27], [28], [29].

b) Variational IB and deep neural nets.: The connection between the IB approach and deep neural nets was first made in [14], in which the authors stated that any DNN can be quantified by the mutual information between the layers and the input and output variables. In addition, the goal of any supervised learning can be translated as an IB problem. Due to the complexity in deriving closed-form solutions, various efforts have been made to obtain algorithmic variational IB solutions, see, for example [15], [30], [31], [22], [32]. The main difference between this paper and the aforementioned works is that we aim to derive *closed-form achievable* bounds for the IB problem, which does *not* need to run an algorithm to measure the performance.

C. Notations and organization of the paper

We denote scalars by lowercase letters and vectors by bold lowercase. For a random variable x defined on the probability space (Ω, \mathcal{F}, p) , we denote $\mathbb{E}[x]$ and $h(x)$ the expectation and differential entropy of x , respectively. For two random variables x and y , we use $I(x; y)$ to denote their mutual information. In this paper, the base of logarithm is the mathematical constant e .

This paper is organized as follows. The system model of the IB problem under study is introduced in Section II. Our main technical results on an achievable closed-form solution to the IB problem is given in Section III. Numerical results are provided in Section IV to validate the proposed IB scheme, on both synthetic and real-world datasets. Finally, conclusion and future perspective are placed in Section V.

II. SYSTEM MODEL

Consider the following binary classification problem: for label $y \in \mathbb{R}$ drawn from a symmetric Bernoulli distribution (that is, $y = \pm 1$ with $\Pr(y = -1) = \Pr(y = 1) = 1/2$), the data vector $\mathbf{x} = (x_1, \dots, x_{d_0}) \in \mathbb{R}^{d_0}$ follows a Gaussian mixture model (GMM) and depends on the label y in such as way that

$$\mathbf{x} = y \cdot \boldsymbol{\beta} + \boldsymbol{\epsilon}, \quad (2)$$

for some *deterministic* vector $\boldsymbol{\beta} = (\beta_1, \dots, \beta_{d_0}) \in \mathbb{R}^{d_0}$ and Gaussian random noise $\boldsymbol{\epsilon} = (\epsilon_1, \dots, \epsilon_{d_0}) \sim \mathcal{N}(\mathbf{0}, \mathbf{I}_{d_0})$. In the context of IB, we are interested in constructing an intermediate representation $\mathbf{t} = (t_1, \dots, t_d) \in \mathbb{R}^d$ of \mathbf{x} that

- (i) contains sufficiently rich information (maximizing $I(y; \mathbf{t})$) on the source random variable y for, say downstream classification; and
- (ii) is a compact (in an information theoretic sense) representation of \mathbf{x} , so that, e.g., the information leakage of \mathbf{x} is small (for secrecy consideration) and/or generalizes better;

by solving the following constrained optimization problem (which is, in fact, an IB problem)

$$\max_{p(\mathbf{t}|\mathbf{x})} I(y; \mathbf{t}) \quad (3a)$$

$$\text{s.t. } I(\mathbf{x}; \mathbf{t}) \leq R, \quad (3b)$$

for some given $R \geq 0$. Here we focus on the setting of $d = d_0$ and, for each $i \in \{1, \dots, d_0\}$, optimize the conditional distribution $p(z_i|x_i)$ by solving the following one-dimensional IB problem,

$$\max_{p(t_i|x_i)} I(y; t_i) \quad (4a)$$

$$\text{s.t. } I(x_i; t_i) \leq R_i, \quad (4b)$$

for some $R_i \geq 0$ such that

$$R_1 + \dots + R_{d_0} = R. \quad (5)$$

In Appendix A, we prove that any achievable solution of (4) is also an achievable solution of the problem in (3); i.e., any $\{p(t_i|x_i) : i \in \{1, \dots, d_0\}\}$ satisfying the constraints (4b) also leads a distribution $p(\mathbf{t}|\mathbf{x})$ satisfying the constraint in (3b).

In the remainder of the paper, we drop the index i for notational convenience.

III. MAIN RESULTS

A closed-form solution to the vanilla IB problem in (4), beyond the case of jointly Gaussian and symmetric Bernoulli (x, y) , to the best of our knowledge, remains an open problem [20].

In an attempt to derive an analytic solution to (4), we propose the following generic form of achievable solution, by introducing the intermediate representation t as

$$t = f_{\text{non-linear}}(x) + n, \quad (6)$$

where $f_{\text{non-linear}} : \mathbb{R} \rightarrow \mathbb{R}$ is a non-linear function, and n is an independent random variable from x , the distribution of which may depend on the non-linear function. Under (6), the objective mutual information writes

$$I(y; t) = h(t) - h(t|y), \quad (7a)$$

$$\begin{aligned} &= - \int_{-\infty}^{\infty} \frac{p(t|y=1) + p(t|y=-1)}{2} \ln \frac{p(t|y=1) + p(t|y=-1)}{2} dt \\ &\quad + \int_{-\infty}^{\infty} \frac{p(t|y=1)}{2} \ln p(t|y=1) dt + \int_{-\infty}^{\infty} \frac{p(t|y=-1)}{2} \ln p(t|y=-1) dt, \end{aligned} \quad (7b)$$

with two conditional probabilities $p(t|y=1)$ and $p(t|y=-1)$ given by

$$\begin{aligned} p(t|y = \pm 1) &= \int_{-\infty}^{\infty} p(x|y = \pm 1) p(t|x) dx \\ &= \int_{-\infty}^{\infty} \frac{1}{\sqrt{2\pi}} \exp\left(-\frac{(x \mp \beta)^2}{2}\right) p_n(t - f_{\text{non-linear}}(x)) dx, \end{aligned} \quad (8)$$

where $p_n(\cdot)$ denotes the probability density function of the random variable n .

In the following, we derive three analytic achievable schemes with different choices of $f_{\text{non-linear}}(\cdot)$ and $p_n(\cdot)$ in (8).

A. An analytic achievable IB solution via one-bit quantization

In this scheme, we employ one-bit quantization as the non-linear function $f_{\text{non-linear}}$ applied on the observation x , and denote $\hat{x} = f_{\text{non-linear}}(x) = \text{sign}(x)$ ¹. This results in a Markov chain: $y \rightarrow x \rightarrow \hat{x} \rightarrow t$. According to the data processing inequality, we have $I(\hat{x}; t) \geq I(x; t)$, leading to a lower bound for the original IB in (4) given by:

$$\max_{p(t|\hat{x})} I(y; t) \tag{9a}$$

$$\text{s.t. } I(\hat{x}; t) \leq R. \tag{9b}$$

It is important to note here that both \hat{x} and source y follow a Bernoulli distribution with equal probability, i.e., $\text{Bern}(1/2)$. This scenario is known as doubly symmetric binary sources (DSBS) and has been thoroughly investigated in the information theory literature. This observation leads to the following result.

Proposition 1 (An achievable solution to IB via one-bit quantization). For the IB problem defined in (9) with symmetric Bernoulli y and $x|y \sim \mathcal{N}(y\beta, 1)$ as in (2), if $0 \leq R \leq \ln 2$, then the optimal rate $I^*(y; t)$ is lower bounded by $I_1(q)$, with q solution to

$$I(\hat{x}; t) = \ln 2 - H(q) = R, \tag{10}$$

where $H(q) = -q \ln(q) - (1 - q) \ln(1 - q)$, and for the ease of notation, we define $I_1(q)$ as the mutual information $I(y; t)$ given q .

Proof of Proposition 1. According to the findings in [19], the optimal design of the representation of \hat{x} for DSBS y and \hat{x} is *explicitly* given by:

$$t = \hat{x} \oplus Q, \quad \text{where } Q \sim \text{Bern}(q) \text{ for some } q \in [0, 1], \tag{11}$$

¹This idea is inspired by that given mixture Gaussian observation x , sign function is one simple approach to reconstruct binary source y

which aligns with the form in (6) and \oplus denotes the exclusive ‘or’ operation. It then follows from (8) that, in this scheme, $I_1(q)$ further simplifies as:

$$I_1(q) = 1 - H(p \star q), \quad p \star q := p(1 - q) + q(1 - p), \quad (12)$$

where p represents the probability of $\hat{x} = 1$ conditioned on $y = -1$. \square

B. An analytic achievable IB solution via deterministic quantization

In the second scheme, we take a different approach than Section III-A, by letting $n = 0$ but applying a more sophisticated non-linear function on the observation x . Precisely, we utilize a deterministic quantizer $\hat{Q}(\cdot)$ ² with L levels to map the observation x into L bins, that is, $t = f_{\text{non-linear}}(x) = \hat{Q}(x)$. The quantization points are denoted as $\{q_i\}_{i=1}^{L-1}$, with $q_0 = -\infty$ and $q_L = \infty$ representing the two extreme points, and t is quantized as T_j for $x \in [q_{j-1}, q_j]$, $\forall j \in \{1, \dots, L\}$.

In this case, the conditional probability in (8) becomes

$$\begin{aligned} p(t = T_j|y) &= p(q_{j-1} \leq x \leq q_j|y) \\ &= Q(q_j - \beta y) - Q(q_{j-1} - \beta y), \quad \forall j \in 1, \dots, L, \end{aligned} \quad (13)$$

with $Q(t) = \int_t^\infty \frac{1}{\sqrt{2\pi}} \exp(-x^2/2) dx$ the Gaussian Q-function.

Since the mapping from x to t is deterministic, the mutual information $I(x; t)$ becomes the entropy of t , i.e., $I(x; t) = H(t)$. This leads to the following lower bound for the original IB in (4) as

$$\max_{\{q_i\}_{i=1}^{L-1}} I(y; t) \quad (14a)$$

$$\text{s.t.} \quad H(t) \leq R. \quad (14b)$$

However, solving analytically the problem in (14) remains challenging. In the following, we derive a lower bound to (14) by setting $H(t) = R$.

Proposition 2 (An achievable solution to IB via deterministic quantization). For the IB problem defined in (14) with symmetric Bernoulli y and $x|y \sim \mathcal{N}(y\beta, 1)$ as in (2), the optimal rate $I^*(y; t)$ is lower bounded by $I_2(\Delta)$, with Δ solution to

$$-(e^{-R} - \Delta) \ln(e^{-R} - \Delta) - ((\lceil e^R \rceil - 1)e^{-R} + \Delta) \ln(e^{-R} + \frac{\Delta}{\lceil e^R \rceil - 1}) = R, \quad (15)$$

²This idea extends the one-bit quantization into L -level quantization without further randomness to simplify the problem.

where for notational simplicity, we denote $I_2(\Delta)$ the mutual information $I(y; t)$ given Δ , and the quantization points $\{q_i\}_{i=1}^{\lceil e^R \rceil}$ can also be obtained based on Δ by

$$p(q_{i-1} \leq x \leq q_i) = \begin{cases} e^R - \Delta & \text{if } i = 1, \\ e^R + \frac{\Delta}{\lceil e^R \rceil - 1} & \text{otherwise.} \end{cases} \quad (16)$$

Proof of Proposition 2. To derive an explicit lower bound to the IB problem in (14), we set $H(t) = R$. This can be achieved by setting the cardinality of the quantization space of t to e^R . If e^R is an integer, we have an alphabet size of e^R with a uniform distribution of e^{-R} . Otherwise, we may set the cardinality of the t -space to $\lceil e^R \rceil$. In this case, using a uniform distribution with $\lceil e^R \rceil$ symbols, we obtain $H(t) > R$. To achieve an entropy of t equal to R , we need to find Δ by solving (15) to tune the quantization probabilities. Finally, in this scheme $I_2(\Delta)$ can be computed using (13) together with (7), and based on quantization points in (16). \square

C. An analytic achievable IB solution via “soft” quantization

In this scheme, we propose to solve the IB problem by using *jointly* tuning the non-linear function (other than quantization) *and* the noise n . The proposed approach involves applying Minimum Mean Square Error (MMSE) estimation to the observation x using the hyperbolic tangent \tanh function, which can be viewed as a “soft” quantization technique. After the MMSE estimation, Gaussian noise is then added to the intermediate representation t as:

$$t = f_{\text{non-linear}}(x) + n = \tanh(\beta x) + n, \quad (17)$$

with $n \sim \mathcal{N}(0, \alpha^{-2})$. In terms of mutual information $I(x; t)$ or $I(y; t)$, this is equivalent to

$$t = \alpha \tanh(\beta x) + \hat{n}, \quad (18)$$

with $\hat{n} \sim \mathcal{N}(0, 1)$. By incorporating these steps, the IB problem can be reformulated as follows:

$$\max_{\alpha \geq 0} I(y; t) \quad (19a)$$

$$\text{s.t. } I(x; t) \leq R, \quad (19b)$$

$$t|x \sim \mathcal{N}(\alpha \tanh(\beta x), 1). \quad (19c)$$

The main ingredients of this scheme is as follows:

- (i) Due to the mathematically involved form of mutual information, we propose two upper bounds of $I(x; t)$, which are then forced to equal R . As such, $I(x; t)$ is upper bounded

by R satisfying the constraint in (19b). The upper bounds on $I(x; t)$ boil down to finding lower bounds on $\ln(\cosh \alpha t)$ by applying the Bernoulli variational distribution of $\tanh \beta x$. Since $\ln(\cosh(x)) \geq \sqrt{1+x^2} - 1$, $\forall x \geq 0$, the first bound can provide an upper bound on $I(x; t)$ for all R , while the second bound is based on $\ln(\cosh(x)) \geq x - \ln 2$, $\forall x \geq 0$, which is tighter than the first lower bound on $\ln(\cosh x)$ for relatively large x , resulting in a tighter upper bound on $I(x; t)$. However, the second bound only holds for $R \geq \ln 2$.

(ii) We then solve the equation where each proposed upper bound of $I(x; t)$ is equal to R , to obtain the *analytic solution* of α .

(iii) Finally, the value of the mutual information $I(y; t)$ is obtained by taking the value of α .

This leads to the following result, the proof of which is given in Appendix B.

Proposition 3 (An achievable solution to IB via soft quantization). For the variational IB problem defined in (19) with symmetric Bernoulli y and $x|y \sim \mathcal{N}(y\beta, 1)$, the optimal rate $I^*(y; t)$ is lower bounded by $\max\{I_3(\alpha_{\text{lb}_1}), I_4(\alpha_{\text{lb}_2})\}$ if $R \geq \ln 2$, and lower bounded by $I_3(\alpha_{\text{lb}_1})$ otherwise, by defining

$$\alpha_{\text{lb}_1} = \sqrt{\frac{(R-1)(1+f(\beta)) + \sqrt{((1+f(\beta))^2 + 4g^2(\beta)(R^2 - 2R))}}{((1+f(\beta))^2 - 4g^2(\beta))/2}}, \quad (20a)$$

$$\alpha_{\text{lb}_2} = \sqrt{\frac{R - \ln 2}{\frac{1}{2} + \frac{f(\beta)}{2} - g(\beta)}}, \quad \text{if } R \geq \ln 2, \quad (20b)$$

where, for the ease of presentation, we define $I_3(\alpha_{\text{lb}_1})$ and $I_4(\alpha_{\text{lb}_2})$ as the mutual information $I(y; t)$ given α_{lb_1} and α_{lb_2} respectively, $\hat{x} := \tanh(\beta x)$, and³

$$f(\beta) = \int_{-1}^1 p(\hat{x}) \hat{x}^2 d\hat{x}, \quad g(\beta) = \int_{-1}^1 p(\hat{x}) |\hat{x}| d\hat{x}. \quad (21a)$$

We discuss the two limiting cases of $R = 0$ and $R \rightarrow \infty$ of Proposition 3 in the following remark.

Remark 1 (Limiting cases). First, for $R = 0$, we have $\alpha_{\text{lb}_1} = 0$ per its definition in (20a). Next, if $R \rightarrow \infty$, it then follows from (20) that both α_{lb_1} and α_{lb_2} reach infinity. Due to the design of the intermediate representation as in (18), if $\alpha \rightarrow \infty$, then we have $t = \hat{x}$, which implies the objective mutual information $I(y; t)$ can attain the optimal value $I(x; y)$. These findings are verified through simulations in Appendix E.

³Note that $f(\beta)$ and $g(\beta)$ are deterministic functions of β .

By combining the three proposed achievable schemes in Proposition 1–3, we obtain the optimally combined achievable scheme, as stated in Theorem 1. This is, to the best of our knowledge, the first time that achievable solutions to the IB problem in (4) are given in an analytic manner.

Theorem 1 (An analytic and achievable scheme to IB under Gaussian mixtures). For the IB problem defined in (4), the optimal rate $I^*(y; t)$ is lower bounded by $\max\{I_1(q), I_2(\Delta), I_3(\alpha_{\text{lb1}}), I_4(\alpha_{\text{lb2}})\}$.

We next provide numerical results to assess the performance of the solutions given in Theorem 1.

IV. NUMERICAL EVALUATIONS AND DISCUSSIONS

In this section, we provide numerical experiments to validate our theoretical results in Theorem 1, on both synthetic data (such as univariate and multivariate Gaussian mixture data) and real-world data (e.g., from the popular MNIST handwritten digit dataset [33] and CIFAR 10 dataset [34]). Despite derived here for GMM data, our approach yields satisfactory performance on real-world *non-Gaussian* features obtained from the MNIST dataset, suggesting possibly wider applicability for the proposed analytic IB scheme.

Numerical results show our proposed closed-form achievable bounds are close to the (numerically) optimal solution of the Blahut-Arimoto (BA) algorithm introduced in [13], not only in the univariate case but also in the multivariate setting, and yield better results compared to existing IB approaches such as the popular Information Dropout method [22].

In the following, we briefly discuss the BA algorithm [13] and the Information Dropout method [22]. These two methods are designed to the following equivalent Lagrange form of the IB problem in (1)

$$\min_{p(t|x)} I(x; t) - \lambda I(y; t), \quad (22)$$

where λ is a predefined tradeoff parameter. Inspired by the rate distortion theory calculation and by discretizing the continuous space of x and t , [13] proposed to apply the BA algorithm [35], [36] to solve the optimization problem in (22) numerically, by alternating among the three probability distributions $p(t)$, $p(y|t)$, and $p(t|x)$, starting from random initialization. With the three distributions, the objective mutual information $I(y; t)$ and $I(x; t)$ can then be computed. [13] also gave a short proof of the convergence of the BA algorithm, which, however, does *not* necessarily imply the uniqueness of the solution.

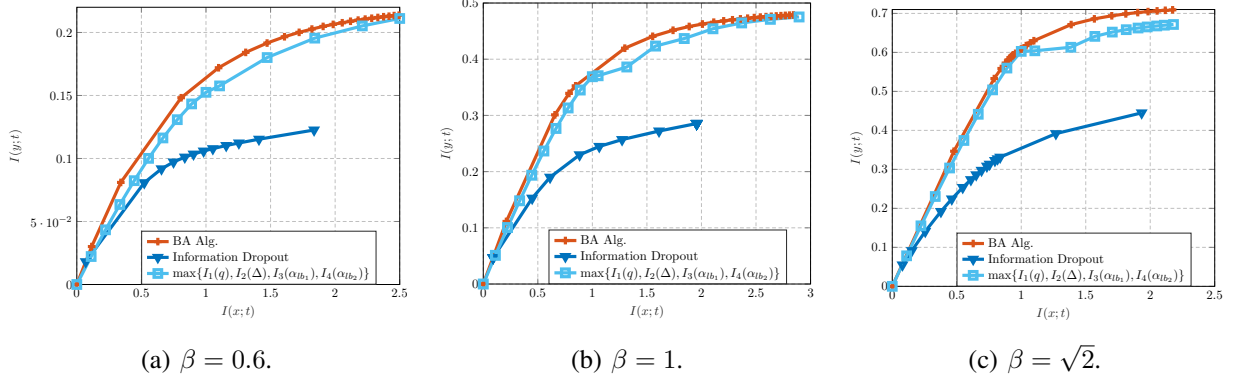


Fig. 1: The three methods compared in terms of the objective mutual information $I(y; t)$ and the constraint $I(x; t)$ for Bernoulli source and univariate mixture Gaussian observation when $\beta = \{0.6, 1, \sqrt{2}\}$.

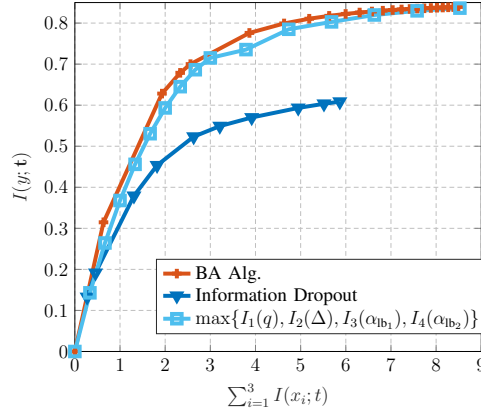


Fig. 2: Three methods compared with the respect to the objective mutual information $I(y; t)$ and the constraint $\sum_{i=1}^3 I(x_i; t_i)$ for Bernoulli source and three-dimensional mixture multivariate Gaussian observation when $\beta = (0.9, 1, 1.1)$.

The Information Dropout method introduced by [22] proposes to design the intermediate representation t as $t = f_1(x) \odot \eta$, where $f_1(x)$ is the output of a fully-connected NN with input x , and η follows the log-normal distribution, i.e., $\eta \sim \log \mathcal{N}(0, f_2^2(x))$, with variance parameter $f_2(x)$ also given by the output of a fully-connected NN with input x . In addition, the network parameters are optimized using gradient descent. Here, we use single-hidden-layer neural network models for both f_1 and f_2 , i.e., $f_1(x) = \sigma(w_1 x) + 1$ and $f_2(x) = \sigma(w_2 x)$, with $\sigma(t) = (1 + \exp(-t))^{-1}$ the logistic sigmoid function. An additional bias term $b = 1$ is added to

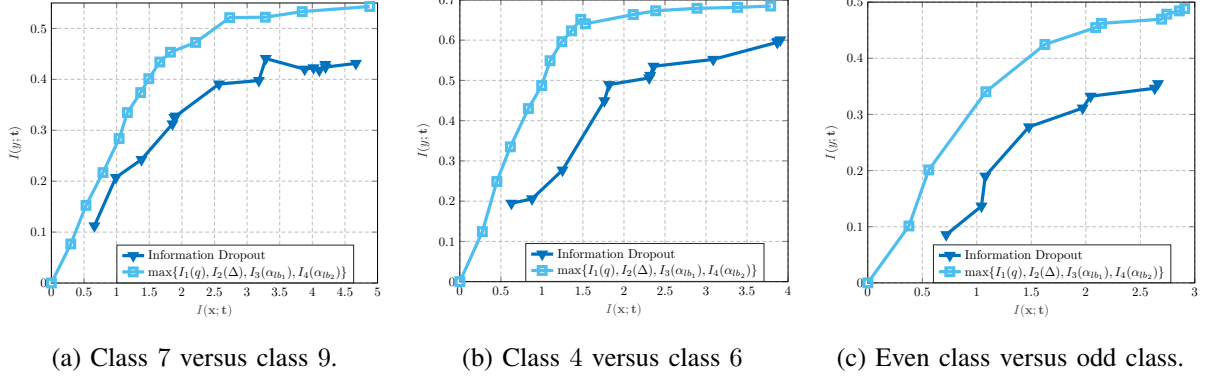


Fig. 3: Two methods compared with the respect to the objective mutual information $I(y; t)$ and the constraint $I(x; t)$ for dimension-reduced MNIST data, (a) class 7 versus class 9, (b) class 4 versus class 6, (c) even class versus odd class

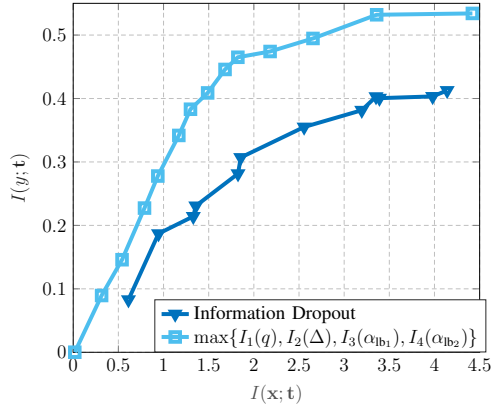


Fig. 4: Two methods compared with the respect to the objective mutual information $I(y; t)$ and the constraint $I(x; t)$ for dimension-reduced CIFAR-10 features from class ‘cat’ versus class ‘deer’.

$f_1(x)$ to avoid 0 for calculating the conditional probability $p(t|x)$. Then, brute-force search (over the space of w_1 and w_2) can be applied to solve the optimization problem in (22), and to further determine $I(y; t)$ and $I(x; t)$. In the simulation, the discretization step in each dimension for all methods is set as $\frac{1}{20}$.

Figure 1 compares the proposed *closed-form* lower bound given in Theorem 1 on the IB optimal rate $I^*(y; t)$, to those obtained from the BA algorithm (which serves as a numerical “proxy” of the IB optimal rate $I^*(y; t)$) and the Information Dropout method, for Bernoulli source

label and *univariate* Gaussian mixture data with different $\beta = \{0.6, 1, \sqrt{2}\}$. Figure 2 extends the above experiments to multivariate setting with $\beta = (0.9, 1.0, 1.1)$, by solving the IB problem in an entry-wise manner. Moreover, for the rate allocation in (5), we set $R_1 = R_2 = R_3 = \frac{R}{3}$ in this section when we consider the case of $d_0 = 3$. In all four figures, we consistently observe a close match between our proposed lower bounds and the numerically optimal BA solution for all R range.

The Information Dropout method performs close to the proposed approach in the small R region, but worse for R large. This also shows that within the Information Dropout framework, the single-hidden-layer NN model, despite being universal approximators with a sufficiently large number of neurons [37], is less efficient in solving the IB problem. This is also (empirically) supported by the fact that some (large) value of mutual information $I(x; t)$ *cannot* be reached with the single-layer Information Dropout approach in Figure 1 and 2.

We also apply the derived analytic IB scheme in Theorem 1 to real-world (so in general non-Gaussian) data drawn from the popular MNIST database [33] and CIFAR-10 dataset [38]. Since it is time consuming to estimate high-dimensional mutual information, we reduce the dimension of the vectorized MNIST images or CIFAR-10 samples by randomly projecting through a random Gaussian matrix to obtain features of dimension $d_0 = 3$. Note that due to the high complexity of the BA algorithm, in our experiments on real-world, we only compare the proposed IB scheme in Theorem 1 and the Information Dropout approach.

Figure 3 and Figure 4 depict the “accuracy-complexity” tradeoff of the proposed analytic IB scheme versus the Information Dropout approach, by comparing the objective mutual information $I(y; \mathbf{t})$ against the budget rate $I(\mathbf{x}; \mathbf{t})$ on dimension-reduced MNIST features⁴ and dimension-reduced CIFAR-10 features⁵ with the aforementioned methods. Since only image samples are practically available, the Jackknife approach [39] is applied to numerically estimate the mutual information $I(y; \mathbf{t})$ and $I(\mathbf{x}; \mathbf{t})$ from the available MNIST and CIFAR-10 image samples. The practical implementation of the BA algorithm needs an additional estimate of the (optimal) conditional distribution $p(\mathbf{t}|\mathbf{x})$ from data samples, and is not performed here for the sake of fair comparison. For better visualization, linear interpolation is adopted to estimate the maximum of two proposed lower bounds in Theorem 3. We see, perhaps surprisingly, that

⁴See Appendix C for the details of MNIST data pre-processing.

⁵See Appendix D for the details of CIFAR-10 data pre-processing.

the advantageous performance of the proposed analytic IB scheme is consistently observed for real-world non-Gaussian data as for (synthetic) Gaussian mixture data, thereby showing possibly wider applicability of the proposed approach.

V. CONCLUSION, LIMITATION, AND FUTURE PERSPECTIVE

In this paper, we provided a closed-form solution to the IB problem with Bernoulli source and Gaussian mixture data. The theoretical result is based on the scalar case, and we further extended it to the multidimensional case. Numerical experiments have been performed to validate the theoretical results.

However, when we extend it to the multidimensional case, the key factor for our proposed methods is $d = d_0$. In this case, there is a gap if we operate on each dimension of \mathbf{x} independently, since some information will be lost. How to optimize in the vector space might be an interesting problem to think about. In addition, considering the case where $d < d_0$, a direct way is to delete some elements in \mathbf{x} that are connected to small β_i to force the dimensions of \mathbf{x} and \mathbf{t} to be equal. It is also an interesting open problem to find better compression strategies than simple deletion.

REFERENCES

- [1] A. Krizhevsky, I. Sutskever, and G. E. Hinton, "ImageNet classification with deep convolutional neural networks," *Communications of the ACM*, vol. 60, no. 6, pp. 84–90, 2017.
- [2] D. Silver, A. Huang, C. J. Maddison, A. Guez, L. Sifre, G. v. d. Driessche, J. Schrittwieser, I. Antonoglou, V. Panneershelvam, M. Lanctot, S. Dieleman, D. Grewe, J. Nham, N. Kalchbrenner, I. Sutskever, T. Lillicrap, M. Leach, K. Kavukcuoglu, T. Graepel, and D. Hassabis, "Mastering the game of Go with deep neural networks and tree search," *Nature*, vol. 529, no. 7587, pp. 484–489, 2016.
- [3] A. Vaswani, N. Shazeer, N. Parmar, J. Uszkoreit, L. Jones, A. N. Gomez, L. u. Kaiser, and I. Polosukhin, "Attention is all you need," in *Advances in Neural Information Processing Systems*, vol. 30. Curran Associates, Inc., 2017. [Online]. Available: <https://proceedings.neurips.cc/paper/2017/file/3f5ee243547dee91fbd053c1c4a845aa-Paper.pdf>
- [4] J. Ho, A. Jain, and P. Abbeel, "Denoising diffusion probabilistic models," in *Advances in Neural Information Processing Systems*, vol. 33. Curran Associates, Inc., 2020, pp. 6840–6851. [Online]. Available: <https://proceedings.neurips.cc/paper/2020/file/4c5bcfec8584af0d967f1ab10179ca4b-Paper.pdf>
- [5] I. Goodfellow, Y. Bengio, and A. Courville, *Deep Learning*, ser. Adaptive Computation and Machine Learning series. MIT Press, 2016. [Online]. Available: <http://www.deeplearningbook.org>
- [6] R. Battiti, "Using mutual information for selecting features in supervised neural net learning," *IEEE Transactions on Neural Networks*, vol. 5, no. 4, pp. 537–550, 1994.
- [7] I. Goodfellow, J. Pouget-Abadie, M. Mirza, B. Xu, D. Warde-Farley, S. Ozair, A. Courville, and Y. Bengio, "Generative Adversarial Nets," in *Advances in Neural Information Processing Systems*, ser. NIPS'14, vol. 27. Curran Associates, Inc., 2014, pp. 2672–2680. [Online]. Available: <https://proceedings.neurips.cc/paper/2014/file/5ca3e9b122f61f8f06494c97b1afccf3-Paper.pdf>

- [8] M. Arjovsky, S. Chintala, and L. Bottou, “Wasserstein generative adversarial networks,” in *Proceedings of the 34th International Conference on Machine Learning*, ser. Proceedings of Machine Learning Research, D. Precup and Y. W. Teh, Eds., vol. 70. PMLR, 06–11 Aug 2017, pp. 214–223. [Online]. Available: <https://proceedings.mlr.press/v70/arjovsky17a.html>
- [9] X. Chen, Y. Duan, R. Houthoofd, J. Schulman, I. Sutskever, and P. Abbeel, “Infogan: Interpretable representation learning by information maximizing generative adversarial nets,” in *Advances in Neural Information Processing Systems*, vol. 29. Curran Associates, Inc., 2016. [Online]. Available: <https://proceedings.neurips.cc/paper/2016/file/7c9d0b1f96aebd7b5eca8c3edaa19ebb-Paper.pdf>
- [10] G. Biau, B. Cadre, M. Sangnier, and U. Tanielian, “Some theoretical properties of GANS,” *The Annals of Statistics*, vol. 48, no. 3, pp. 1539–1566, 2020.
- [11] R. D. Hjelm, A. Fedorov, S. Lavoie-Marchildon, K. Grewal, P. Bachman, A. Trischler, and Y. Bengio, “Learning deep representations by mutual information estimation and maximization,” in *International Conference on Learning Representations*, 2019. [Online]. Available: <https://openreview.net/forum?id=Bklr3j0cKX>
- [12] P. Bachman, R. D. Hjelm, and W. Buchwalter, “Learning representations by maximizing mutual information across views,” in *Advances in Neural Information Processing Systems*, vol. 32. Curran Associates, Inc., 2019. [Online]. Available: <https://proceedings.neurips.cc/paper/2019/file/ddf354219aac374f1d40b7e760ee5bb7-Paper.pdf>
- [13] N. Tishby, F. C. Pereira, and W. Bialek, “The information bottleneck method,” *arXiv*, 2000.
- [14] N. Tishby and N. Zaslavsky, “Deep Learning and the Information Bottleneck Principle,” in *2015 IEEE Information Theory Workshop (ITW)*, ser. 2015 IEEE Information Theory Workshop (ITW), 2015, pp. 1–5.
- [15] A. A. Alemi, I. Fischer, J. V. Dillon, and K. Murphy, “Deep variational information bottleneck,” in *International Conference on Learning Representations*, 2017. [Online]. Available: <https://openreview.net/forum?id=HyxQzBceg>
- [16] R. Shwartz-Ziv and N. Tishby, “Opening the black box of deep neural networks via information,” *arXiv preprint arXiv:1703.00810*, 2017.
- [17] A. M. Saxe, Y. Bansal, J. Dapello, M. Advani, A. Kolchinsky, B. D. Tracey, and D. D. Cox, “On the information bottleneck theory of deep learning,” *Journal of Statistical Mechanics: Theory and Experiment*, vol. 2019, no. 12, p. 124020, 2019.
- [18] R. A. Amjad and B. C. Geiger, “Learning representations for neural network-based classification using the information bottleneck principle,” *IEEE transactions on pattern analysis and machine intelligence*, vol. 42, no. 9, pp. 2225–2239, 2019.
- [19] A. Zaidi, I. Estella-Aguerrí, and S. Shamai, “On the information bottleneck problems: Models, connections, applications and information theoretic views,” *Entropy*, vol. 22, no. 2, p. 151, 2020.
- [20] Z. Goldfeld and Y. Polyanskiy, “The Information Bottleneck Problem and its Applications in Machine Learning,” *IEEE Journal on Selected Areas in Information Theory*, vol. 1, no. 1, pp. 19–38, 2020.
- [21] C. M. Bishop, *Pattern Recognition and Machine Learning*, 1st ed., ser. Information Science and Statistics. Springer-Verlag New York, 2006. [Online]. Available: <https://www.springer.com/cn/book/9780387310732>
- [22] A. Achille and S. Soatto, “Information Dropout: Learning Optimal Representations Through Noisy Computation,” *IEEE transactions on pattern analysis and machine intelligence*, vol. 40, no. 12, pp. 2897–2905, 2018.
- [23] N. Slonim and N. Tishby, “Agglomerative Information Bottleneck,” in *Advances in Neural Information Processing Systems*, vol. 12. MIT Press, 1999.
- [24] A. Makhdoumi, S. Salamatian, N. Fawaz, and M. Médard, “From the information bottleneck to the privacy funnel,” in *2014 IEEE Information Theory Workshop (ITW 2014)*, 2014, pp. 501–505.
- [25] S. Asodeh and F. P. Calmon, “Bottleneck problems: An information and estimation-theoretic view,” *Entropy*, vol. 22, no. 11, 2020.
- [26] H. Hsu, S. Asodeh, S. Salamatian, and F. P. Calmon, “Generalizing bottleneck problems,” in *2018 IEEE International Symposium on Information Theory (ISIT)*, 2018, pp. 531–535.

- [27] S. Kung, “Compressive Privacy: From Information\Estimation Theory to Machine Learning [Lecture Notes],” *IEEE Signal Processing Magazine*, vol. 34, no. 1, pp. 94–112, Jan. 2017.
- [28] B. Rodríguez-Gálvez, R. Thobaben, and M. Skoglund, “A Variational Approach to Privacy and Fairness,” in *2021 IEEE Information Theory Workshop (ITW)*, Oct. 2021, pp. 1–6.
- [29] Y. Bu, T. Wang, and G. W. Wornell, “SDP Methods for Sensitivity-Constrained Privacy Funnel and Information Bottleneck Problems,” in *2021 IEEE International Symposium on Information Theory (ISIT)*, Jul. 2021, pp. 49–54.
- [30] M. Chalk, O. Marre, and G. Tkacik, “Relevant sparse codes with variational information bottleneck,” *Advances in Neural Information Processing Systems*, vol. 29, 2016.
- [31] B. Dai, C. Zhu, B. Guo, and D. Wipf, “Compressing neural networks using the variational information bottleneck,” in *International Conference on Machine Learning*. PMLR, 2018, pp. 1135–1144.
- [32] I. Higgins, L. Matthey, A. Pal, C. Burgess, X. Glorot, M. Botvinick, S. Mohamed, and A. Lerchner, “beta-VAE: Learning basic visual concepts with a constrained variational framework,” in *International Conference on Learning Representations*, 2017.
- [33] Y. LeCun, L. Bottou, Y. Bengio, and P. Haffner, “Gradient-based learning applied to document recognition,” *Proceedings of the IEEE*, vol. 86, no. 11, pp. 2278–2324, 1998.
- [34] A. Krizhevsky, V. Nair, and G. Hinton, “Cifar-10 (canadian institute for advanced research).” [Online]. Available: <http://www.cs.toronto.edu/~kriz/cifar.html>
- [35] R. Blahut, “Computation of channel capacity and rate-distortion functions,” *IEEE Transactions on Information Theory*, vol. 18, no. 4, pp. 460–473, 1972.
- [36] S. Arimoto, “An algorithm for computing the capacity of arbitrary discrete memoryless channels,” *IEEE Transactions on Information Theory*, vol. 18, no. 1, pp. 14–20, 1972.
- [37] K. Hornik, “Approximation capabilities of multilayer feedforward networks,” *Neural Networks*, vol. 4, no. 2, pp. 251–257, 1991. [Online]. Available: <https://www.sciencedirect.com/science/article/pii/089360809190009T>
- [38] A. Krizhevsky, G. Hinton *et al.*, “Learning multiple layers of features from tiny images,” 2009.
- [39] X. Zeng, Y. Xia, and H. Tong, “Jackknife approach to the estimation of mutual information,” *Proceedings of the National Academy of Sciences*, vol. 115, no. 40, pp. 9956–9961, 2018. [Online]. Available: <https://www.pnas.org/doi/abs/10.1073/pnas.1715593115>
- [40] T. M. Cover and J. A. Thomas, *Elements of Information Theory (2nd edition)*. Hoboken, NJ: Wiley, 2006.
- [41] P. Chen, G. Chen, and S. Zhang, “Log hyperbolic cosine loss improves variational auto-encoder,” 2018.

APPENDIX A

ACHIEVABILITY PROOF OF (4)

In order to prove that a solution of (4) is also a solution of (3), we only need to prove

$$I(\mathbf{x}; \mathbf{t}) \leq \sum_{i \in [1:d_0]} I(x_i; t_i), \quad (23)$$

where $t_i \mid x_i \sim \mathcal{N}(\alpha_i \tanh(\beta x_i), 1)$. This is because by (4), we have $\sum_{i \in [1:d_0]} I(x_i; t_i) = \sum_{i \in [1:d_0]} R_i = R$. If (23) holds, we also have $I(\mathbf{x}; \mathbf{t}) \leq R$, coinciding with the secrecy constraint in (3b). In the rest of this section, we will prove (23).

By our construction in (4), it can be seen that for each $i \in [1 : d_0]$, we have the following Markov chain

$$(x_1, t_1, x_2, t_2, \dots, x_{i-1}, t_{i-1}, x_{i+1}, t_{i+1}, \dots, x_{d_0}, t_{d_0}) \longrightarrow x_i \longrightarrow t_i. \quad (24)$$

By the chain rule of mutual information, we have

$$I(\mathbf{x}; \mathbf{t}) = I(\mathbf{x}; t_1) + I(\mathbf{x}; t_2 | t_1) + \dots + I(\mathbf{x}; t_{d_0} | t_1, \dots, t_{d_0-1}). \quad (25)$$

We then focus on each term on the RHS of (25). For each $i \in [1 : d_0]$, we have

$$I(\mathbf{x}; t_i | t_1, \dots, t_{i-1}) = I(x_i; t_i | t_1, \dots, t_{i-1}) + I(x_1, \dots, x_{i-1}, x_{i+1}, \dots, x_{d_0}; t_i | x_i, t_1, \dots, t_{i-1}) \quad (26a)$$

$$= I(x_i; t_i | t_1, \dots, t_{i-1}) \quad (26b)$$

$$\leq I(x_i, t_1, \dots, t_{i-1}; t_i) \quad (26c)$$

$$= I(x_i; t_i) + I(t_1, \dots, t_{i-1}; t_i | x_i) \quad (26d)$$

$$= I(x_i; t_i), \quad (26e)$$

where (26b) and (26e) come from the Markov chain (24). By taking (26e) into (25), we can directly prove (23).

APPENDIX B

PROOF OF PROPOSITION 3

Since \hat{x} is a one-to-one mapping of x , we have

$$I(x; t) = h(t) - h(t|x) = h(t) - h(t|\hat{x}) = I(\hat{x}; t). \quad (27)$$

Since $t|\hat{x}$ is a Gaussian distribution with unit variance, the conditional differential entropy is $h(t|\hat{x}) = \frac{1}{2} \ln(2\pi e)$. In addition, we can compute the probability of \hat{x} as

$$\begin{aligned} p(\hat{x}) &= p(x) \frac{\partial x}{\partial \hat{x}}, \\ &= \frac{1}{\beta \sqrt{2\pi}} \exp\left(-\frac{(1/\beta \tanh^{-1}(\hat{x}))^2 + \beta^2}{2}\right) \frac{1}{(1-\hat{x}^2)^{1.5}}. \end{aligned} \quad (28)$$

By the information inequality [40], for any probability distribution $q(t)$, we have

$$h(t) = - \int p(t) \ln(p(t)) dt \leq - \int p(t) \ln(q(t)) dt. \quad (29)$$

Then by (27) and (29), we can derive an upper bound of $I(\hat{x}; t)$ based on variational distribution $q(t)$,

$$I(\hat{x}; t) \leq - \int p(t) \ln(q(t)) dt - \frac{1}{2} \ln(2\pi e). \quad (30)$$

Moreover, the distribution of t is much complicated due to the distribution of \hat{x} in (28). Therefore, instead of introducing variational distribution of t , we come up with the variational distribution \hat{x} . Since \hat{x} is the MMSE Estimation of y given observation x , for simplicity, we design the variational distribution of \hat{x} as Bernoulli distribution, i.e., $q(\hat{x} = -1) = q(\hat{x} = 1) = \frac{1}{2}$. Intuitively speaking, the less the noise power of x is, the closer the variational distribution $q(\hat{x})$ gets to true distribution $p(\hat{x})$. Therefore, the variational distribution of t is given by

$$q(t) = \int_{-1}^1 p(t|\hat{x}) q(\hat{x}) d\hat{x}, \quad (31a)$$

$$= \frac{1}{\sqrt{2\pi}} \exp\left(-\frac{t^2 + \alpha^2}{2}\right) (\cosh(\alpha t)). \quad (31b)$$

Hence, by taking (31b) into (30), we have

$$I(\hat{x}; t) \leq - \int_{-\infty}^{\infty} \left(\int_{-1}^1 p(t|\hat{x}) p(\hat{x}) d\hat{x} \right) \ln q(t) dt - \frac{1}{2} \ln(2\pi e), \quad (32a)$$

$$= \frac{\alpha^2 - 1}{2} + \underbrace{\int_{-1}^1 p(\hat{x}) \left(\int_{-\infty}^{\infty} p(t|\hat{x}) \frac{t^2}{2} dt \right) d\hat{x}}_{(c)} - \int_{-\infty}^{\infty} \left(\int_{-1}^1 p(t|\hat{x}) p(\hat{x}) d\hat{x} \right) \ln(\cosh(\alpha t)) dt. \quad (32b)$$

Since $t|\hat{x}$ follows a Gaussian distribution $\mathcal{N}(\alpha\hat{x}, 1)$, then (c) in (32b) is given by

$$\begin{aligned} \int_{-1}^1 p(\hat{x}) \left(\int_{-\infty}^{\infty} p(t|\hat{x}) \frac{t^2}{2} dt \right) d\hat{x} &= \int_{-1}^1 p(\hat{x}) \frac{1 + \alpha^2 \hat{x}^2}{2} d\hat{x}, \\ &= \frac{1}{2} + \frac{\alpha^2}{2} f(\beta). \end{aligned} \quad (33)$$

By taking (33) into (32b), we have

$$I(\hat{x}; t) \leq \frac{\alpha^2}{2} (1 + f(\beta)) - \int_{-\infty}^{\infty} \left(\int_{-1}^1 p(t|\hat{x}) p(\hat{x}) d\hat{x} \right) \ln(\cosh(\alpha t)) dt. \quad (34)$$

The RHS of (34) is hard to compute in closed-form due to the term $\ln(\cosh \alpha t)$. Hence, in the following we will propose three lower bounds of $\ln(\cosh \alpha t)$ to derive a loosen lower bound of $I(\hat{x}; t)$ with respect to (34).

First lower bound of $\ln(\cosh \alpha t)$. By $\ln(\cosh(x)) \geq \sqrt{1+x^2} - 1$, $\forall x \geq 0$, we have

$$\begin{aligned} & - \int_{-1}^1 p(\hat{x}) \int_{-\infty}^{\infty} \frac{1}{\sqrt{2\pi}} \exp\left(-\frac{(t-\alpha\hat{x})^2}{2}\right) \ln(\cosh(\alpha t)) dt d\hat{x} \\ & \leq - \int_{-1}^1 p(\hat{x}) \int_{-\infty}^{\infty} \frac{1}{\sqrt{2\pi}} \exp\left(-\frac{(t-\alpha\hat{x})^2}{2}\right) \left[\sqrt{1+\alpha^2 t^2} - 1\right] dt d\hat{x}, \\ & \leq - \int_{-1}^1 p(\hat{x}) \left[\sqrt{1+\alpha^4 \hat{x}^2}\right] d\hat{x} + 1, \end{aligned} \quad (35a)$$

$$= - \int_{-1}^0 2p(\hat{x}) \left[\sqrt{1+\alpha^4 \hat{x}^2}\right] d\hat{x} + 1, \quad (35b)$$

where (35a) comes from the convexity of function $f(t) = \sqrt{1+\alpha^2 t^2}$, i.e., $\mathbb{E}[\sqrt{1+\alpha^2 t^2}] \geq \sqrt{1+\alpha^2(\mathbb{E}[t])^2}$, and (35b) follows since $p(\hat{x})$ and $\sqrt{1+\alpha^4 \hat{x}^2}$ are both even functions regarding to \hat{x} .

Furthermore, by $\int_{-1}^0 2p(\hat{x}) d\hat{x} = 1$, we have

$$\int_{-1}^0 2p(\hat{x}) \hat{x} d\hat{x} = -g(\beta). \quad (36)$$

Based on the Jensen's inequality, an upper bound of the RHS of (35b) is given by

$$- \int_{-1}^0 2p(\hat{x}) \left[\sqrt{1+\alpha^4 \hat{x}^2}\right] d\hat{x} + 1 \leq \sqrt{1+\alpha^4 \left(\int_{-1}^0 2p(\hat{x}) \hat{x} d\hat{x}\right)^2} + 1, \quad (37a)$$

$$= -\sqrt{1+\alpha^4 (g(\beta))^2} + 1. \quad (37b)$$

By taking (37b) and (35b) into (34), we obtain the following upper bound of $I(\hat{x}; t)$,

$$I(\hat{x}; t) \leq \frac{\alpha^2}{2} (1 + f(\beta)) - \sqrt{1+\alpha^4 (g(\beta))^2} + 1, \quad (38)$$

the RHS of which will be then forced to equal R , i.e.,

$$\frac{\alpha^2}{2} (1 + f(\beta)) - \sqrt{1+\alpha^4 (g(\beta))^2} + 1 = R. \quad (39)$$

The next step is to solve the equation (39). Assuming that $x = \alpha^2$, $a = \frac{(1+f(\beta))^2 - 4(g(\beta))^2}{4}$, $b = (1-R)(1+f(\beta))$, $c = R^2 - 2R$. and $\Delta = b^2 - 4ac$. First in order to check whether there exists a real solution, we need to check whether Δ is always non-negative when $R \geq 0$. Then we have

$$\Delta = (1 + f(\beta))^2 + 4(g(\beta))^2 (R^2 - 2R) \quad (40a)$$

$$\geq (1 + f(\beta))^2 + 4(g(\beta))^2 (-1) \quad (40b)$$

$$= (1 + f(\beta) - 2(g(\beta)))(1 + f(\beta) + 2(g(\beta))). \quad (40c)$$

Note that the term $1 + f(\beta) + 2(g(\beta))$ in (40c) is always non-negative, and based on (36), the term $1 + f(\beta) - 2(g(\beta))$ can be further developed as

$$\begin{aligned}
 1 + f(\beta) - 2(g(\beta)) &= 1 + 2 \int_{-1}^0 p(\hat{x}) \hat{x}^2 d\hat{x} + 4 \int_{-1}^0 p(\hat{x}) \hat{x} d\hat{x}, \\
 &= 1 + 2 \int_{-1}^0 p(\hat{x}) [(\hat{x} + 1)^2 - 1] d\hat{x}, \\
 &> 1 + 2 \int_{-1}^0 p(\hat{x}) (-1) d\hat{x}, \\
 &= 0.
 \end{aligned} \tag{41}$$

Hence, the term $1 + f(\beta) - 2(g(\beta))$ is always positive, and thus $\Delta \geq 0$ holds when $R \geq 0$. Therefore, there always exists some real solution of (39).

Secondly, we need to check whether there exists a positive solution in problem (39). From (41), it can be seen that a is always positive. When $0 \leq R \leq 1$, b is also positive. In this way, we need to compare $-b$ and $\sqrt{\Delta}$, so we have

$$b^2 - \Delta = (R^2 - 2R) \underbrace{[(1 + f(\beta))^2 - 4(g(\beta))^2]}_{(d)}. \tag{42}$$

Therefore, since (d) in (42) is always positive, when $0 \leq R \leq 2$, $R^2 - 2R$ is non-positive, it results in $\|b\| \leq \sqrt{\Delta}$ while $R \geq 2$, it comes to $\|b\| \geq \sqrt{\Delta}$.

As a result, when $R \leq 1$, we have $\|b\| \leq \sqrt{\Delta}$ and $-b + \sqrt{\Delta} \geq 0$; thus there exists one positive and real solution of (39), which is

$$\alpha_{lb_1} = \sqrt{\frac{-b + \sqrt{\Delta}}{2a}}. \tag{43}$$

In addition, when $R > 1$, we have $-b$ is positive and $\sqrt{\Delta}$ is also positive; thus there always exists some positive solution of (39). However, it may exist two positive solutions. Since the larger correlation factor α will result in the larger $I(y; t)$, we will choose the larger solution when two positive solutions occur. Therefore, the solution is also

$$\alpha_{lb_1} = \sqrt{\frac{-b + \sqrt{\Delta}}{2a}}. \tag{44}$$

Second lower bound of $\ln(\cosh \alpha t)$. By $\ln(\cosh(x)) \geq x - \ln 2, \forall x \geq 0$ [41], separating the negative part and positive part of t and denoting p as an auxiliary variable of $t - \alpha \hat{x}$, i.e., $p = t - \alpha \hat{x}$, we have

$$\begin{aligned} & - \int_{-\infty}^{\infty} \left(\int_{-1}^1 p(t|\hat{x}) p(\hat{x}) d\hat{x} \right) \ln(\cosh(\alpha t)) dt \\ & \leq - \int_{-1}^1 p(\hat{x}) \left(\int_{-\infty}^0 p(t|\hat{x}) [-\alpha t - \ln 2] dt \right) d\hat{x} - \int_{-1}^1 p(\hat{x}) \left(\int_0^{\infty} p(t|\hat{x}) [\alpha t - \ln 2] dt \right) d\hat{x}, \end{aligned} \quad (45a)$$

$$\begin{aligned} & = - \int_{-1}^1 p(\hat{x}) \left(\int_{-\infty}^{-\alpha \hat{x}} \frac{1}{\sqrt{2\pi}} \exp\left(-\frac{p^2}{2}\right) [-\alpha(p + \alpha \hat{x})] dp \right) d\hat{x} - \int_{-1}^1 p(\hat{x}) \left(\int_{-\alpha \hat{x}}^{\infty} \frac{1}{\sqrt{2\pi}} \exp\left(-\frac{p^2}{2}\right) [\alpha(p + \alpha \hat{x})] dp \right) d\hat{x} + 1. \end{aligned} \quad (45b)$$

Moreover, using that fact that $\int \exp(-\frac{p^2}{2}) p dp = -\exp(-\frac{p^2}{2})$, and separating the negative part and positive part of \hat{x} , (45b) is further developed as

$$\begin{aligned} & \ln 2 - \frac{2\alpha}{\sqrt{2\pi}} \int_{-1}^1 p(\hat{x}) \exp\left(-\frac{\alpha^2 \hat{x}^2}{2}\right) d\hat{x} - \int_{-1}^1 p(\hat{x}) [-\alpha^2 \hat{x}] \int_{-\infty}^{-\alpha \hat{x}} \frac{1}{\sqrt{2\pi}} \exp\left(-\frac{p^2}{2}\right) dp d\hat{x} \\ & \quad - \int_{-1}^1 p(\hat{x}) [\alpha^2 \hat{x}] \int_{-\alpha \hat{x}}^{\infty} \frac{1}{\sqrt{2\pi}} \exp\left(-\frac{p^2}{2}\right) dp d\hat{x}, \end{aligned} \quad (46a)$$

$$\begin{aligned} & = \ln 2 - \frac{2\alpha}{\sqrt{2\pi}} \int_{-1}^1 p(\hat{x}) \exp\left(-\frac{\alpha^2 \hat{x}^2}{2}\right) d\hat{x} + \frac{\alpha^2}{\sqrt{2\pi}} \int_{-1}^0 \hat{x} p(\hat{x}) \left[\int_{\alpha \hat{x}}^{-\alpha \hat{x}} \exp\left(-\frac{p^2}{2}\right) dp \right] d\hat{x} \\ & \quad + \frac{\alpha^2}{\sqrt{2\pi}} \int_0^1 \hat{x} p(\hat{x}) \left[- \int_{-\alpha \hat{x}}^{\alpha \hat{x}} \exp\left(-\frac{p^2}{2}\right) dp \right] d\hat{x}, \end{aligned} \quad (46b)$$

$$\begin{aligned} & = \ln 2 - \frac{2\alpha}{\sqrt{2\pi}} \int_{-1}^1 p(\hat{x}) \exp\left(-\frac{\alpha^2 \hat{x}^2}{2}\right) d\hat{x} + \underbrace{2\alpha^2 \int_{-1}^0 \hat{x} p(\hat{x}) \left[\int_{\alpha \hat{x}}^{-\alpha \hat{x}} \frac{1}{\sqrt{2\pi}} \exp\left(-\frac{p^2}{2}\right) dp \right] d\hat{x}}_{(e)}. \end{aligned} \quad (46c)$$

Suppose that a random variable $P \sim \mathcal{N}(0, 1)$ follows unit Gaussian distribution. For any non-negative real number α and negative real number $\hat{x} < 0$, we have the following inequality

$$\Pr(P \geq -\alpha \hat{x}) = \int_{-\alpha \hat{x}}^{\infty} \frac{1}{\sqrt{2\pi}} \exp\left(-\frac{p^2}{2}\right) dp, \quad (47a)$$

$$\leq \int_{-\alpha \hat{x}}^{\infty} \frac{1}{\sqrt{2\pi}} \frac{p}{-\alpha \hat{x}} \exp\left(-\frac{p^2}{2}\right) dp, \quad (47b)$$

$$= \frac{1}{\alpha \hat{x} \sqrt{2\pi}} \left(-\exp\left(-\frac{\alpha^2 \hat{x}^2}{2}\right) \right). \quad (47c)$$

Based on the inequality (47), we can derive an upper bound on (e) in (46c) as

$$(e) = 2\alpha^2 \int_{-1}^0 p(\hat{x})\hat{x} [1 - 2\Pr(P \geq (-a\hat{x}))] d\hat{x}, \quad (48a)$$

$$\leq 2\alpha^2 \int_{-1}^0 p(\hat{x})\hat{x} \left[1 - \frac{2}{\alpha\hat{x}\sqrt{2\pi}} \left(-\exp\left(-\frac{\alpha^2\hat{x}^2}{2}\right) \right) \right] d\hat{x} \quad (48b)$$

Hence, by taking (48b) into (46c) and combining (34), we can further relax the constraint and obtain the following upper bound on $I(\hat{x}; t)$

$$I(\hat{x}; t) \leq \ln 2 + 2\alpha^2 \int_{-1}^0 p(\hat{x})\hat{x} d\hat{x} + \frac{\alpha^2}{2}(1 + f(\beta)), \quad (49a)$$

$$= \alpha^2 \left[\frac{1}{2} + \frac{f(\beta)}{2} - g(\beta) \right] + \ln 2, \quad (49b)$$

the RHS of which will be then forced to equal R , i.e.,

$$\underbrace{\alpha^2 \left[\frac{1}{2} + \frac{f(\beta)}{2} - g(\beta) \right]}_{(f)} + \ln 2 = R. \quad (50)$$

According to (41), the term (f) in (50) is always positive. Therefore, when $R \geq \ln 2$, there exists a positive solution to (50), which is

$$\alpha_{\text{lb}_2} = \sqrt{\frac{R - \ln 2}{\frac{1}{2} + \frac{f(\beta)}{2} - g(\beta)}} \quad (51)$$

In the end, through (7) we can compute the lower bound on $I(y; t)$, i.e., $I_3(\alpha_{\text{lb}_1})$, and $I_4(\alpha_{\text{lb}_2})$, respectively.

APPENDIX C

MNIST DATA PRE-PROCESSING

Recall that our theoretical results assume that the input data $\mathbf{x} \in \mathbb{R}^{d_0}$ are drawn from the following symmetric binary Gaussian mixture model

$$\mathcal{C}_1 : \mathbf{x} \sim \mathcal{N}(-\boldsymbol{\beta}, \mathbf{I}_{d_0}), \quad \mathcal{C}_2 : \mathbf{x} \sim \mathcal{N}(+\boldsymbol{\beta}, \mathbf{I}_{d_0}). \quad (52)$$

For vectorized MNIST images of dimension $p = 784$ composed of ten classes (number 0 to 9), here we choose the images of number 7 versus 9 to perform binary classification. For the sake of computational complexity, we apply a random projection that reduce the 784-dimensional raw data vector $\tilde{\mathbf{x}}$ to obtain a three-dimensional feature \mathbf{x} , i.e., $\mathbf{x} = \mathbf{W}\tilde{\mathbf{x}} \in \mathbb{R}^3$, with the i.i.d. entries of $\mathbf{W} \in \mathbb{R}^{3 \times 783}$ following a standard Gaussian distribution. Then, we collect three-dimensional feature matrices $\mathbf{X}_1 \in \mathbb{R}^{3 \times n_1}$ and $\mathbf{X}_2 \in \mathbb{R}^{3 \times n_2}$ of class \mathcal{C}_1 and \mathcal{C}_2 , and we perform

further pre-processing to make them closer to (52). First, the empirical means of each class are computed as $\hat{\boldsymbol{\mu}}_1 = \frac{1}{n_1} \mathbf{X}_1 \mathbf{1}_{n_1}$ and $\hat{\boldsymbol{\mu}}_2 = \frac{1}{n_2} \mathbf{X}_2 \mathbf{1}_{n_2}$. We then compute the empirical covariances as $\hat{\mathbf{C}}_1 = \frac{1}{n_1} (\mathbf{X}_1 - \hat{\boldsymbol{\mu}}_1 \mathbf{1}_{n_1}^\top)(\mathbf{X}_1 - \hat{\boldsymbol{\mu}}_1 \mathbf{1}_{n_1}^\top)^\top$ and similarly for \mathbf{X}_2 . Finally, whitened features matrices are obtained via

$$\tilde{\mathbf{X}}_1 = \frac{1}{2}(\hat{\boldsymbol{\mu}}_1 - \hat{\boldsymbol{\mu}}_2) + \hat{\mathbf{C}}_1^{-\frac{1}{2}}(\mathbf{X}_1 - \hat{\boldsymbol{\mu}}_1 \mathbf{1}_{n_1}^\top), \quad (53)$$

for class \mathcal{C}_1 and similarly $\tilde{\mathbf{X}}_2$ for class \mathcal{C}_1 . In the simulation, we choose 2000 samples of each class to estimate mutual information using Jackknife approach.

APPENDIX D

CIFAR-10 DATA PRE-PROCESSING

In order to preprocess the CIFAR-10 dataset, we adopt a similar approach as that used for the MNIST dataset. Firstly, we extract features from the CIFAR-10 dataset using a feature module in the pre-trained VGG16 model. The extracted features transform the data from the resized dimension $\mathbb{R}^{3 \times 224 \times 224}$ to the dimension $\mathbb{R}^{512 \times 7 \times 7}$. Next, we normalize each dimension of the vectorized features based on the maximum value of each dimension across all datasets. However, since estimating high-dimensional mutual information is computationally complex and time-consuming, we apply a random projection to reduce the 25088-dimensional normalized feature vector $\tilde{\mathbf{x}}$ to obtain a three-dimensional feature vector \mathbf{x} , i.e., $\mathbf{x} = \mathbf{W}\tilde{\mathbf{x}} \in \mathbb{R}^3$, where each entry of $\mathbf{W} \in \mathbb{R}^{3 \times 25088}$ follows an independent standard Gaussian distribution. We choose the cat class and the deer class from the CIFAR-10 dataset for this simulation. Following the same preprocessing steps used for the MNIST dataset, we collect the three-dimensional feature matrices $\mathbf{X}_k \in \mathbb{R}^{3 \times n_k}, \forall k \in \{1, 2\}$, and compute the empirical means of each class $\hat{\boldsymbol{\mu}}_k, \forall k \in \{1, 2\}$, as well as the empirical covariance matrix $\hat{\mathbf{C}}_k, \forall k \in \{1, 2\}$. Using (53), we obtain the whitened feature matrices $\tilde{\mathbf{X}}_k, \forall k \in \{1, 2\}$ in the simulation. In the simulation, we estimate the mutual information using the Jackknife approach with 2000 samples of each class.

APPENDIX E

FURTHER DISCUSSIONS ON LIMITING CASES IN PROPOSITION 3

In Figure 5, we present, following the discussions in Remark 1, numerical behaviors of the two proposed lower bounds at the extreme points where R is rather large and $R = 0$, for both $\beta = 1$ and $\beta = \sqrt{2}$. We observe that:

- (i) for $R = 0$, we have $\alpha_{lb_1} = 0$ (per its definition in (20a) as already discussed in Remark 1, so that $I_3(\alpha_{lb_1}) = 0$; and
- (ii) as $R \rightarrow \infty$, we have that both α_{lb_1} and α_{lb_2} reach infinity, so that both lower bounds $I_3(\alpha_{lb_1})$ and $I_4(\alpha_{lb_2})$ converge to the optimal point of $I(x; y)$.

This thus provides numerical evidence for the statement made in Remark 1.

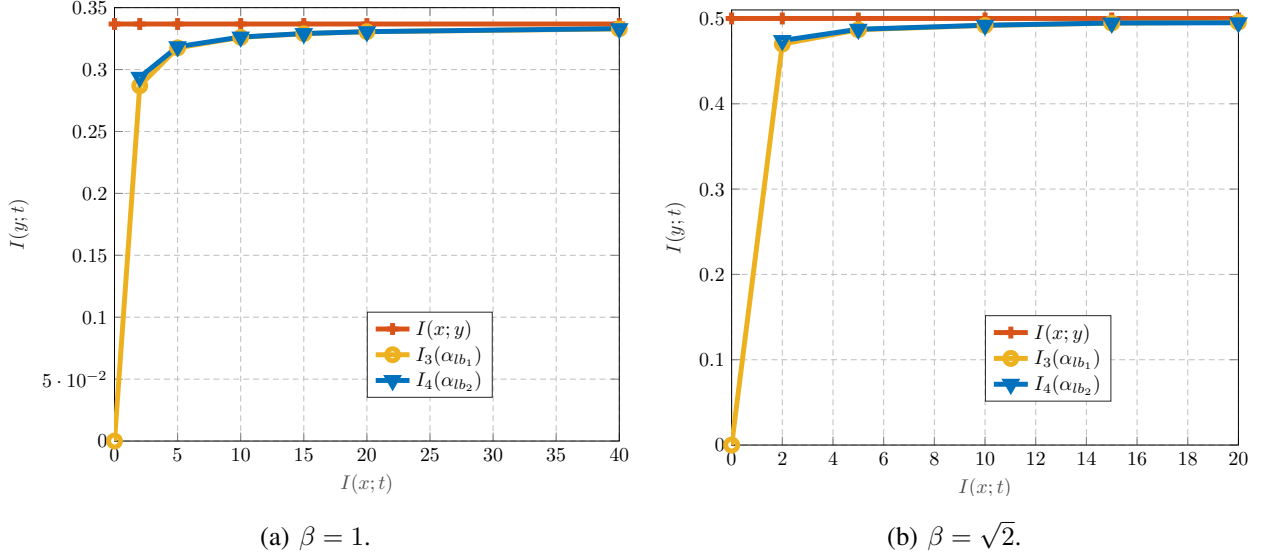


Fig. 5: The objective mutual information $I(y; t)$ versus the constraint $I(x; t)$ for two proposed lower bounds $I_3(\alpha_{lb_1})$ and $I_4(\alpha_{lb_2})$ when $\beta \in \{1, \sqrt{2}\}$.